Communication

Monitoring Horseradish Peroxidase Activity with a Nanopore Detector

Yuri Ivanov *, Alexander Ableev, Ivan Shumov, Irina Ivanova, Nikita Vaulin, Denis Lebedev, Anton Bukatin, Ivan Mukhin, Alexander Archakov

Posted Date: 22 August 2023

doi: 10.20944/preprints202308.1511.v1

Keywords: nanopore detector; solid-state nanopore; horseradish peroxidase; enzymatic activity

Communication

Monitoring Horseradish Peroxidase Activity with a Nanopore Detector

Yuri D. Ivanov [1], Alexander N. Ableev [1], Ivan D. Shumov [1], Irina A. Ivanova [1], Nikita V. Vaulin [2], Denis V. Lebedev [2], Anton S. Bukatin [2], Ivan S. Mukhin [2] and Alexander I. Archakov [1]

[1] Institute of Biomedical Chemistry, Moscow, Russia
[2] Alferov Federal State Budgetary Institution of Higher Education and Science Saint Petersburg National Research Academic University of the Russian Academy of Sciences, St. Petersburg, Russia
* Correspondence: yurii.ivanov.nata@gmail.com (Yu.D.I).

Abstract: We demonstrate the use of a nanotechnology-based approach for the investigation of enzymatic activity of a single molecule of horseradish peroxidase with a solid-state nanopore. The artificial 5 nm solid-state nanopore has been formed in a 40-nm-thick silicon nitride structure. Single molecule of HRP has been entrapped into the nanopore. The activity of horseradish peroxidase (HRP) enzyme molecule inserted in the nanopore has been monitored by recording the time dependence of the ion current through the nanopore in the course of the reaction of 2,2'-azino-bis(3-ethylbenzothiazoline-6-sulfonate) (ABTS) oxidation reaction. We have found that in the process of ABTS oxidation in the presence of 2.5 mM hydrogen peroxide, individual HRP enzyme molecules are able to retain activity for approximately 700 seconds before a decrease in the ion current through the nanopore, which can be explained by structural changes of the enzyme.

Keywords: nanopore detector; solid-state nanopore; horseradish peroxidase; enzymatic activity

1. Introduction

Nanotechnology-based approaches are becoming widely utilized in single-molecule studies of enzymes. These approaches include atomic force microscopy (AFM) is commonly employed for estimation of activity of single enzyme molecules. For instance, in [1], semi-contact mode of AFM was used for the monitoring of height fluctuations of lysozyme molecules adsorbed on mica. The time dependencies of the height fluctuations were obtained without scanning, upon positioning the AFM tip above lysozyme monolayer under various conditions: in buffer, in the presence of the lysozyme substrate, and in the presence of its inhibitor. The height fluctuations with an amplitude of 1 nm and a period of 50 ms were observed in the presence of the oligosaccharide substrate. In contrast, in the presence of the inhibitor, the fluctuations amplitude reduced to the level observed before the substrate addition. The interpretation of these findings suggests that the height fluctuations of lysozyme correspond to its conformational changes during hydrolysis reaction. Furthermore, these fluctuations can be influenced by differences in height and elasticity of the lysozyme-substrate transition complex. Similar approach was employed in other studies [2,3], in which the fluctuations of IgG antibodies, and the functioning of the chitosanase enzyme were investigated. These examples illustrate how AFM allows one to monitor enzymatic activity by tracking the oscillation of the AFM probe. Furthermore, analogous approach was employed in order to measure the activity of single molecules of cytochrome P450 BM3 enzyme [4].

With respect to AFM, one should emphasize that the implementation of this approach requires expensive equipment, and the AFM experiments are time-consuming. Alternative nanotechnology-based approach to the registration of functioning of single enzyme molecules is based on the use of nanopores. In numerous papers, the use of natural nanopores was reported [5–10]. The approach employing natural nanopores has certain limitations, which are connected with the size of these nanopores. This is why the use of natural nanopores for studying a wide range of enzymes is still limited.

Preprints (www.preprints.org) | NOT PEER-REVIEWED | Posted: 22 August 2023 doi:10.20944/preprints202308.1511.v1

In contrast to the use of natural nanopores, the application of artificial solid-state nanopores overcomes the above-discussed limitation, since their diameters can be varied upon the nanopore fabrication, thus allowing one to study diverse enzymes. Thus, the technology based on solid-state nanopores with a pore diameter of about 5 nm is the most promising nanopore-based approach for investigating enzyme activity [11]. These solid-state nanopores can be fabricated by different methods, including focused ion beam (FIB) [11], controlled dielectric breakdown (SDB) [12,13], and electron beam drilling (EBD) [14]. The material commonly used for the fabrication of solid-state nanopores is silicon nitride (SixNy, hereafter abbreviated SiN).

Enzyme systems play key roles in diverse metabolic processes in living organisms [15]. Herein, horseradish peroxidase (HRP) enzyme, which pertains to a broad class of peroxidases, has been selected as an object owing to its well-known properties. HRP participates in catalytic oxidation reactions involving a wide range of organic and inorganic compounds in the presence of hydrogen peroxide [16]. The molecular weight of HRP is approximately 40 kDa [17]. The catalytic activity of HRP can be assessed using a distinctive reaction involving its substrate 2,2′-azino-bis(3-ethylbenzothiazoline-6-sulfonate) (ABTS) and hydrogen peroxide, described by Sanders et al. [18].

In our present research, the EBD technology has been employed in order to fabricate the solid-state nanopore in SiN. The HRP enzyme was inserted into the nanopore, and the ABTS oxidation reaction was started by adding hydrogen peroxide (H_2O_2). The change in the current flowing through the nanopore during the enzyme functioning has been monitored.

2. Results

2.1. Nanopore fabrication

According to [19], the dimensions of horseradish peroxidase (HRP) were determined to be approximately 4.3×4.8×5.8 nm based on X-ray data [19]. The nanopore with a diameter of 5 nm was fabricated in 40-nm-thick SiN. Figure 1 displays characteristic transmission electron microscopy (TEM) image of the so-fabricated nanopore.

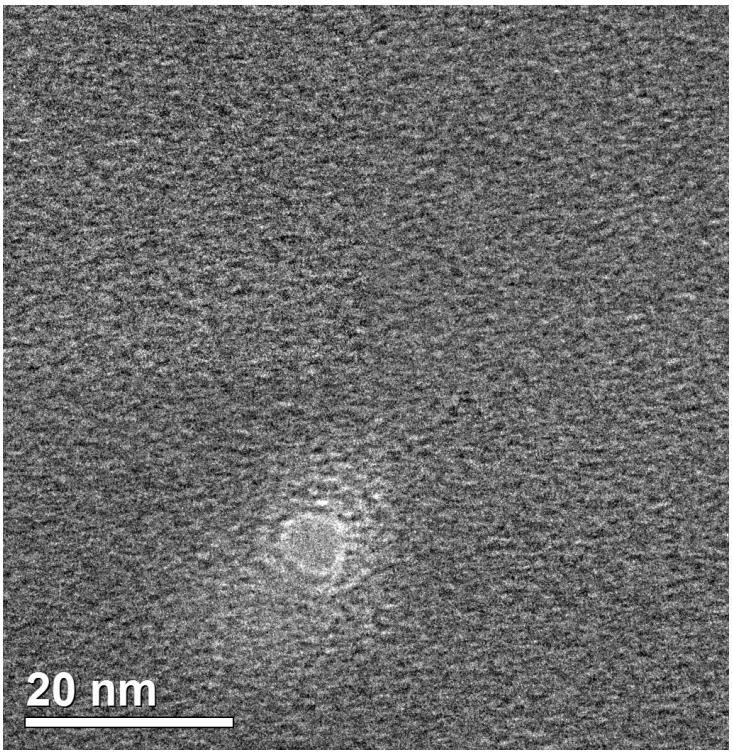

Figure 1. Characteristic TEM image of a nanopore formed by EBD.

Preprints (www.preprints.org) | NOT PEER-REVIEWED | Posted: 22 August 2023 doi:10.20944/preprints202308.1511.v1

The nanopore was observed to have a size slightly smaller than the maximum size of HRP (5.8 nm), but larger than its minimum size (4.3 nm). Accordingly, the nanopore was suitable for accommodating the HRP molecule, preventing it from passing through, while allowing for its incorporation within the nanopore.

2.2. Testing of Nanopore Performance

For the registration of the HRP enzymatic activity with the nanopore-based detector, tests were performed in order to assess the successful incorporation of HRP into the nanopore. Prior to these tests, the chip was washed with ultrapure water measurements. Subsequently, both chambers of the measuring cell were filled with 2 mM PBS-D buffer.

Control experiments were conducted in order to obtain the time dependence of the ion current through the nanopore at a voltage of -200 mV. Pure buffer was initially added to the cis chamber, followed by the addition of ABTS at a concentration of 0.3 mM. Half of the solution volume was then evacuated from the cis chamber, and 0.003% H_2O_2 solution was added. In this experiment, we observed no significant changes in the current signal fluctuations, which remained below 50 pA.

2.3. Nanopore Experiments

For the experiments involving HRP incorporation, a buffer solution containing HRP at a concentration of 10^{-8} M was introduced into the cis part of the cuvette, while the trans part was filled with HRP-free buffer solution. Figure 2 illustrates the ion current dependencies over time during the addition of the corresponding solution to the cis part of the measuring cell.

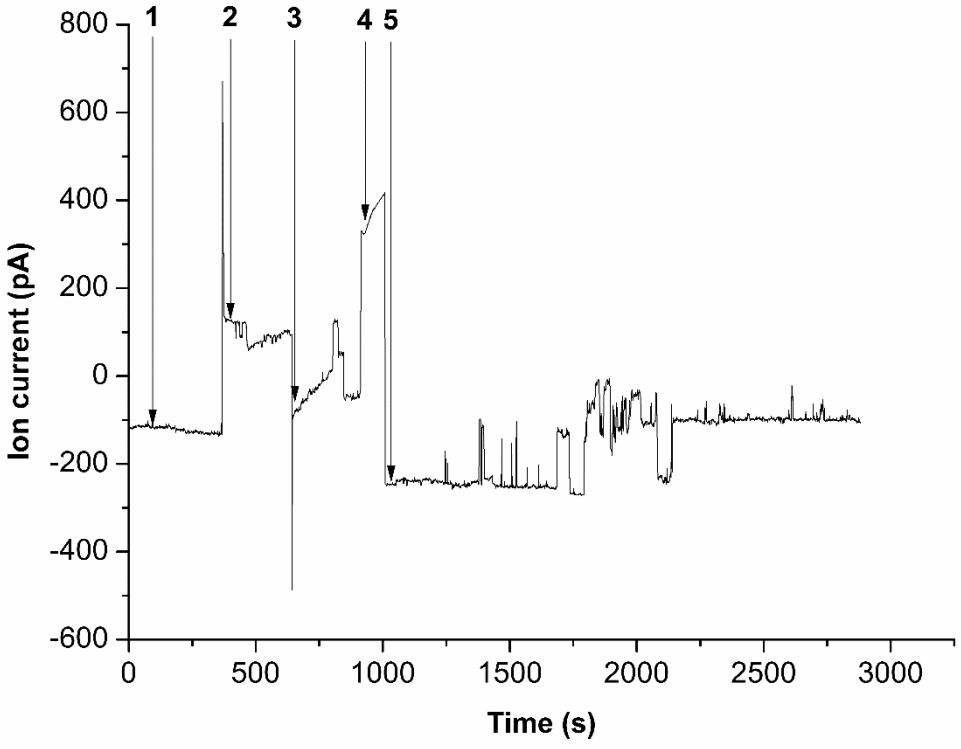

Figure 2. Time dependence of the ion current in through the nanopore. Arrows indicate (1) - addition of 10^{-8} M HRP, voltage U=-200 mV; (2) – voltage polarity switching to U=200 mV; (3) – voltage polarity switching to U=-200 mV; (4) – addition of 0.3 mM ABTS, voltage U=-200 mV; (5) – addition of H_2O_2, voltage U=-200 mV.

The curve shown in Figure 2 indicates that at 10^{-8} M HRP concentration and U=-200 mV voltage applied to the cell (cis-chamber/trans-chamber), the ion current through the nanopore was approximately -100 pA. It should be noted that HRP, at the pH of the buffer solution used, carries a negative charge, which directs the enzyme into the nanopore under the applied voltage conditions.

 doi:10.20944/preprints202308.1511.v1

The voltage polarity was then switched to U=200 mV (cis-chamber/trans-chamber), resulting in a change in the current flowing through the nanopore. At that, the current reached approximately 100 pA. Then the cell polarity was switched again to U=-200 mV (cis-chamber/trans-chamber), forcing the nanopore blockade, as the ion current decreased to zero. The cell was subsequently filled with ABTS solution. After subsequent evacuation of half of the ABTS solution volume, H_2O_2 was added to initiate the ABTS oxidation reaction. This led to a series of significant signal fluctuations, which persisted for about 1800 seconds, indicating the enzyme functioning.

In the spectrophotometry experiments, we observed that under the conditions described in section 4.4, the absorbance of the solution containing 1 nM HRP, reached the value of 0.4 after five minutes of ABTS oxidation reaction. This indicated that the enzyme is able to catalyze the ABTS oxidation in 2 mM PBS-D buffer, i.e. is active. No change in the solution absorbance was observed in blank spectrophotometry experiments in the absence of the enzyme.

3. Discussion

Our study demonstrates the successful use of a 5 nm SiN solid-state nanopore for the monitoring the enzymatic activity of a single HRP molecule. The latter was inserted into the nanopore. In our experiments, the time dependence of the ion current through the nanopore during the enzyme catalytic cycle was recorded. During the catalytic cycle, current pulses were observed, indicating changes in the nanopore size. The latter can be attributed to alterations in the shape of the enzyme molecule confined within the nanopore. These current fluctuations persisted for a considerably long (1800 seconds) time, and after this the enzyme was found to be still active. At that, after 1700 seconds (i.e. approximately 700 seconds after the addition of H_2O_2), a decrease in the ion current was observed. This decrease can be explained by structural changes in the enzyme, leading to a substantial nanopore blockade and thus hindering the ion flow and decreasing the current. These findings demonstrate that individual HRP enzyme molecules are able to retain activity for approximately 700 seconds before undergoing structural changes, which decrease the nanopore conductivity. Control experiments were carried out without the enzyme. In the control experiments, we observed no significant current fluctuations in the presence of ABTS and H_2O_2 were in the measuring cell. These results hold significant implications for comprehending enzyme functionality and enable the analysis of enzyme behaviour at the single-molecule level.

4. Materials and Methods

4.1. Chemicals and Enzyme

The enzyme (peroxidase from horseradish; Cat. #6782) and its substrate ABTS were purchased from Sigma. The experiments were performed in 2 mM Dulbecco's modified phosphate buffered saline (hereafter PBS-D buffer) with a pH of 7.4. Ultrapure deionized water, obtained with a Simplicity UV system (Millipore, Molsheim, France), was used in all experiments. The HRP enzyme was purchased from Sigma (USA). The solution containing 0.3 mM ABTS was prepared by dissolving 8.2 mg of ABTS in 50 mL of in 2 mM PBS-D immediately prior to the experiments. Hydrogen peroxide (H_2O_2) solution was diluted with 2 mM PBS-D to a final concentration in the cell of 0.003% (v/v).

4.2. Nanopore-based detector

The nanopore was formed by EBD in a SiN chip. Its diameter was approximately 5 nm, and its thickness was ~40 nm. This nanopore was obtained with a JEM 2100F high-resolution transmission electron microscope. The nanopore-based detector comprised the measuring cell, which was divided into two chambers with the SiN nanopore integrated into the partition. That is, the chip with the nanopore served as the partition between the two chambers (cis- and trans-). The cell was washed with ultrapure water immediately prior to the measurements.

4.3. Electrical measurements

The both chambers (cis- and trans-) were filled with 700 μL of 2 mM PBS-D (pH 7.4). In the measurements, voltage was applied to the both chambers, and the current flowing through the nanopore was recorded. Ag/AgCl electrodes were immersed into the cis- and trans-chambers in order to apply the electric voltage for recording the ion current through the nanopore. The detector was shielded with a Faraday cell. The current flowing through the nanopore was measured with a patch-clamp amplifier with an intrinsic noise level of 0.3 fA in a frequency band of 1000 Hz. The voltage was varied within the range from -300 to 300 mV. The current signal from the nanopore was recorded at a frequency of 10 kHz using a 16-bit analog-to digital converter (ADC). This signal was then filtered through a low-pass Butterworth filter with a frequency of 1000 Hz. After the measurement cycle, the SiN chip was washed with ultrapure water in order to eliminate salt residues, and reinstalled into the measuring cell.

4.4. Spectrophotometry

Spectrophotometry measurements were performed according to the modified technique reported by Sanders et al. [18]. In the originally reported technique, the measurements are performed in phosphate-citrate buffer [18]. According to Drozd et al. [20], phosphate buffers can also be successfully employed, but the pH should be acidic (5.0) in order to achieve optimal performance [21].

Accordingly, our spectrophotometry measurements were aimed at finding out whether HRP is able to catalyze the oxidation of ABTS by H_2O_2 in 2 mM PBS-D buffer employed in the nanopore-based detector. That is, the modification of the technique consisted in the use of the PBS-D buffer instead of the phosphate-citrate one. Other experimental conditions were similar to those recommended by Sanders et al. [18]. Namely, the concentrations of the enzyme, ABTS and H_2O_2 were 1 nM, 0.3 mM and 2.5 mM, respectively, and the absorbance of the solution was recorded at 405 nm wavelength in 1-cm-long quartz cell. An Agilent 8453 spectrophotometer was used in the measurements. The time dependencies of the absorption were recorded for five minutes in at least three technical replicates.

5. Conclusions

In the course of the research a nanopore (a diameter of approximately 5 nm) with an immobilized HRP was fabricated. The experiments conducted revealed that this nanopore can be successfully used for monitoring the enzymatic activity of a single HRP molecule (which was confined within the nanopore) against its substrate ABTS in the presence of H_2O_2. Importantly, 1800 seconds exhibited observable current fluctuations during enzyme functioning, which were notably absent in the absence of ABTS and H_2O_2. These findings provide valuable insights into the fundamental mechanisms governing enzyme function at the single-molecule level.

Author Contributions: Conceptualization, Yu.D.I. and A.I.A.; methodology, Yu.D.I., A.N.A., and I.S.M.; software, A.N.A; validation, I.D.S.; formal analysis, Yu.D.I.; investigation, Yu.D.I., A.N.A., I.D.S., I.A.I., N.V.V., D.V.L., and I.S.M.; resources, N.V.V., D.V.L., and I.S.M.; data curation, A.N.A., N.V.V., and I.D.S.; writing—original draft preparation, Yu.D.I., A.N.A., and I.D.S.; writing—review and editing, Yu.D.I.; visualization, I.S.M. and I.D.S.; supervision, A.I.A.; project administration, Yu.D.I.; funding acquisition, A.I.A. All authors have read and agreed to the published version of the manuscript.

Funding: The work was performed (done, carried out) within the framework of the Program for Basic Research in the Russian Federation for a long-term period (2021-2030) (No. 122030100168-2).

Data Availability Statement: Correspondence and requests for materials should be addressed to Y.D.I.

Acknowledgments: The AFM measurements were performed employing a Titanium multimode atomic force microscope, which pertains to “Avogadro” large-scale research facilities.

Conflicts of Interest: The authors declare no conflict of interest.

References

1. Radmacher, M.; Fritz, M.; Hansma, H.G.; Hansma, P.K. Direct observation of enzyme activity with the atomic force microscope. *Science* **1994**, *265 (5178)*, 1577-1579. DOI: 10.1126/science.8079171.
2. Thomson, N.H.; Fritz, M.; Radmacher, M.; Cleveland, J.P.; Schmidt, Ch.F.; Hansma, P.K. Protein tracking and detection of protein motion using atomic force microscopy. *Biophys J.* **1996**, *70*, 2421–2431. DOI: 10.1016/S0006-3495(96)79812-0.
3. Arnoldi, M.; Schäffer, T.E.; Fritz, M.; Radmacher, M. Direct observation of single catalytic events of chitosanase by atomic force microscopy. *J. AZoNano — Online J. Nanotechnol*. **2005**, *1 (a108)*, 1-11. DOI : 10.2240/azojono0107.
4. Ivanov, Y.D.; Bukharina, N.S.; Pleshakova, T.O.; Frantsuzov, P.A.; Krokhin, N.V.; Ziborov, V.S.; Archakov, A.I. Atomic force microscopy visualization and measurement of the activity and physicochemical properties of single monomeric and oligomeric enzymes. *BIOPHYSICS* **2011**, *56*, 892–896. https://doi.org/10.1134/S000635091105006X.
5. Sheng, Y.; Zhang, S.; Liu, L.; Wu, H.-C. Measuring enzymatic activities with nanopores. *ChemBioChem* **2020**, *21 (15)*, 2089–2097. https://doi.org/10.1002/cbic.202000079.
6. Chen, H.; Lin, Y.; Long, Y.-T.; Minteer, S.D.; Ying, Y.-L. Nanopore-based measurement of the interaction of P450cam monooxygenase and putidaredoxin at the single-molecule level. *Faraday Discuss*. **2022**, *233*, 295–302. https://doi.org/10.1039/D1FD00042J.
7. Willems, K.; van Meervelt, V.; Wloka, C.; Maglia, G. Single-molecule nanopore enzymology. *Phil. Trans. R. Soc*. B. **2017**, *372 (1726)*, 20160230. https://doi.org/10.1098/rstb.2016.0230.
8. Wloka, C.; van Meervelt, V.; Gelder, D.V.; Danda, N.; Jager, N.; Williams, C.P.; Maglia, G. Label-free and real-time detection of protein ubiquitination with a biological nanopore. *ACS Nano* **2017**, *11 (5)*, 4387–4394. https://doi.org/10.1021/acsnano.6b07760.
9. Pham, B.; Eron, S.J.; Hill, M.E.; Li, X.; Fahie, M.A.; Hardy, J.A.; Chen, M. A nanopore approach for analysis of caspase-7 activity in cell lysates. *Biophys. J*. **2019**, *117 (5)*, 844-855. https://doi.org/10.1016/j.bpj.2019.07.045.
10. Fahie, M.A.; Pham, B.; Li, F.; Chen, M. A selective activity-based approach for analysis of enzymes with an OmpG nanopore. *Methods in Molecular Biology*. **2021**, *2186*, 115–133. https://doi.org/10.1007/978-1-0716-0806-7_9.
11. Li, J.; Stein, D.; McMullan, C.; Branton, D.; Aziz, M.J.; Golovchenko, J.A. Ion-beam sculpting at nanometre length scales. *Nature* **2001**, *412*, 166–169. https://doi.org/10.1038/35084037.
12. Kwok, H.; Briggs, K.; Tabard-Cossa, V. Nanopore fabrication by controlled dielectric breakdown. *PLoS One*. **2014**, *9 (3)*, pp. e92880. https://doi.org/10.1371/journal.pone.0092880.
13. Waugh, M.; Briggs, K.; Gunn, D.; Gibeault, M.; King, S.; Ingram, Q.; Jimenez, A.M.; Berryman, S.; Lomovtsev, D.; Andrzejewski, L.; Tabard-Cossa, V. Solid-state nanopore fabrication by automated controlled breakdown. *Nature Protocols* **2020**, *15 (1)*, 122-143. https://doi.org/10.1038/s41596-019-0255-2.
14. Nam, S.W.; Rooks, M.J.; Kim, K.-B.; Rossnagel, S.M. Ionic field effect transistors with sub-10 nm multiple nanopores. *Nano Lett*. **2009**, *9 (5)*, 2044-2048. https://doi.org/10.1021/nl900309s.
15. Metzler, D.E. Biochemistry: The Chemical Reactions of Living Cells; Academic Press: Oxford, UK, 1970.
16. Rogozhin, V.V.; Kutuzova, G.D.; Ugarova, N.N. Inhibition of horseradish peroxidase by N-ethylamide of o-sulfobenzoylacetic acid. *Bioorganic Chem.* **2000**, *26(2)*, 156-160. https://doi.org/10.1007/BF02759160.
17. Davies, P.F.; Rennke, H.G.; Cotran, R.S. Influence of molecular charge upon the endocytosis and intracellular fate of peroxidase activity in cultured arterial endothelium. *J. Cell Sci*. **1981**. *49 (1)*, 69-86. https://doi.org/10.1242/jcs.49.1.69.
18. Sanders, S.A.; Bray, R.C.; Smith, A.T. pH-dependent properties of a mutant horseradish peroxidase isoenzyme C in which Arg38 has been replaced with lysine. *Eur. J. Biochem*. **1994**, *224*, 1029–1037. https://doi.org/10.1111/j.1432-1033.1994.01029.x.
19. Berglund, G.I.; Carlsson, G.H.; Smith, A.T.; Szöke, H.; Henriksen A.; Hajdu, J. The catalytic pathway of horseradish peroxidase at high resolution. *Nature* **2002**, *417*, 463–468. https://doi.org/10.1038/417463a.
20. Drozd, M.; Pietrzak, M.; Parzuchowski, P.G.; Malinowska, E. Pitfalls and capabilities of various hydrogen donors in evaluation of peroxidase-like activity of gold nanoparticles. *Anal. Bioanal. Chem*. **2016**, *408*, 8505–8513. https://doi.org/10.1007/s00216-016-9976-z.
21. Enzymatic Assay of Peroxidase (EC 1.11.1.7) 2,20-Azino-Bis(3-Ethylbenzthiazoline-6-Sulfonic Acid) as a Substrate Sigma Prod. No. P-6782. Available online: https://www.sigmaaldrich.com/RU/en/technical-

 doi:10.20944/preprints202308.1511.v1

documents/protocol/protein-biology/enzymeactivity-assays/enzymatic-assay-of-peroxidase-abts-as-substrate (accessed on 18 February 2022).